

ATLAS Measurements of CP Violation and Rare Decays in Beauty Mesons

W. Walkowiak

on behalf of the ATLAS Collaboration
 University of Siegen, 57068 Siegen, Germany

The ATLAS experiment at the Large Hadron Collider (LHC) has performed accurate measurements of mixing and CP violation in the neutral B mesons, and also of rare processes happening in electroweak FCNC-suppressed neutral B-mesons decays. This contribution focuses on the latest results from ATLAS, including measurements of rare processes $B_s^0 \rightarrow \mu^+\mu^-$ and $B^0 \rightarrow \mu^+\mu^-$, and measurements of CP violation in $B_s^0 \rightarrow J/\psi\phi$.

I. INTRODUCTION

New physics beyond the Standard Model (SM) may manifest itself in the branching fractions of very rare B meson decays or CP-violating parameters in B_s^0 oscillations. The ATLAS experiment [1] at the Large Hadron Collider (LHC) [2] at CERN performs indirect searches for New Physics by measuring the branching fractions of the rare decays $B_s^0 \rightarrow \mu^+\mu^-$ and $B^0 \rightarrow \mu^+\mu^-$ and the CP-violating phase ϕ_s as well as $\Delta\Gamma_s$ in the $B_s^0 \rightarrow J/\psi\phi$ decay. In addition, projections for the branching fractions of the rare decays $B_{(s)}^0 \rightarrow \mu^+\mu^-$ and expected sensitivities for the search for CP violation in the decay channel $B_{(s)}^0 \rightarrow J/\psi\phi$ at the High-Luminosity LHC (HL-LHC) [3] are presented¹.

II. BRANCHING FRACTIONS OF $B_s^0 \rightarrow \mu^+\mu^-$ AND $B^0 \rightarrow \mu^+\mu^-$

The rare decays $B_s^0 \rightarrow \mu^+\mu^-$ and $B^0 \rightarrow \mu^+\mu^-$, which are sensitive to New Physics in the decays via loop diagrams, are highly suppressed in the Standard Model (SM) with predicted branching fractions [4] of $(3.65 \pm 0.23) \times 10^{-9}$ and $(1.06 \pm 0.09) \times 10^{-10}$, respectively. The ATLAS Run 1 result [5] is compatible with the SM at $\sim 2\sigma$ level, and the $\mathcal{B}(B_{(s)}^0 \rightarrow \mu^+\mu^-)$ values are lower than the CMS-LHCb combined result [6]. A recent LHCb measurement [7] including a part of Run 2 data sets an upper limit of $\mathcal{B}(B^0 \rightarrow \mu^+\mu^-) < 3.4 \times 10^{-10}$ at 95% confidence level (CL) which reduces the tension in this parameter.

The updated ATLAS measurement [8] of the $B_{(s)}^0 \rightarrow \mu^+\mu^-$ branching fractions includes 36.2 fb^{-1} of data taken at a centre-of-mass energy of 13 TeV during 2015 and 2016 (LHC Run 2) and a combination with the result based on 25 fb^{-1} data taken at 7-8 TeV during LHC Run 1. For Run 2, events triggered by two muons ($p_T(\mu_1) > 6 \text{ GeV}$, $p_T(\mu_2) > 4 \text{ GeV}$, $|\eta| < 2.5$)

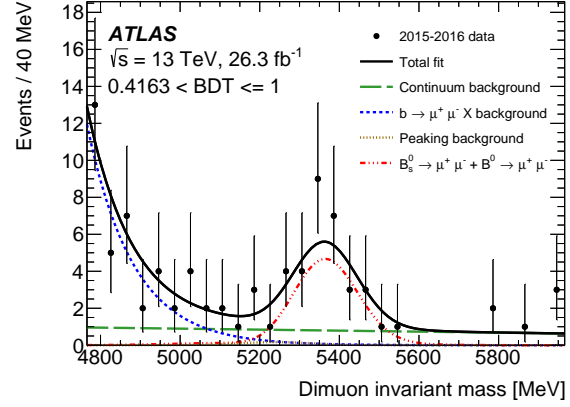


FIG. 1. Dimuon invariant mass distribution in the unblinded data, for the highest interval of BDT output. The result of the maximum-likelihood fit is superimposed. The total fit is shown as a continuous line, with the dashed lines corresponding to the observed signal component, the $b \rightarrow \mu^+\mu^-X$ background, and the continuum background. The signal components are grouped in one single curve, including both the $B_s^0 \rightarrow \mu^+\mu^-$ and the (negative) $B^0 \rightarrow \mu^+\mu^-$ component. The curve representing the peaking $B_{(s)}^0 \rightarrow hh'$ background lies very close to the horizontal axis [8].

with the invariant di-muon mass $m_{\mu^+\mu^-}$ in the range of 4 to 8.5 GeV are selected. The dominant combinatorial background ($b \rightarrow \mu X \times \bar{b} \rightarrow \mu X$ pairs) is rejected by a 15-variable Boosted Decision Tree (BDT) which is trained and tested on data sidebands and simulated signal events. Tails from partially reconstructed $b \rightarrow \mu^+\mu^-X$ decays like $B \rightarrow \mu^+\mu^-X$, $B \rightarrow c\mu X \rightarrow s(d)\mu^+\mu^-X$ or $B_c \rightarrow J/\psi\mu\nu$, which involve real di-muons at low $m_{\mu^+\mu^-}$, and semi-leptonic decays ($B_{(s)}/\Lambda_b^0 \rightarrow h\mu\nu$ with $h = \pi, K, p$) contribute to the signal region and are taken into account in the signal fit. A small contribution of $B \rightarrow hh'$ ($h^{(\prime)} = \pi^\pm, K^\pm$) decays, with hadrons misidentified as muons, peaks in the $B_{(s)}^0 \rightarrow \mu^+\mu^-$ signal region contributing 2.9 ± 2.0 events after a “tight” muon selection is applied. The yield in the normalisation channel $B^\pm \rightarrow J/\psi K^\pm$ with $J/\psi \rightarrow \mu^+\mu^-$ is determined by an unbinned maximum likelihood fit to

¹ Copyright 2019 CERN for the benefit of the ATLAS Collaboration CC-BY-4.0 license.

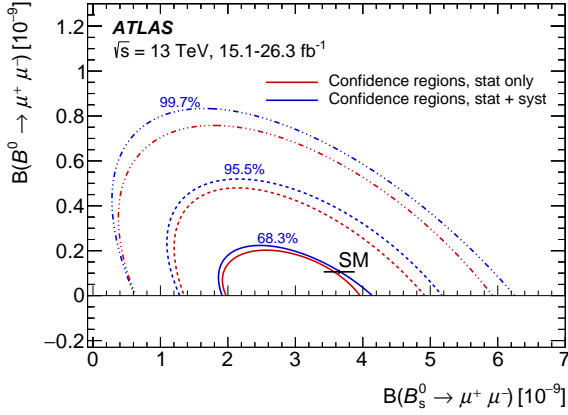


FIG. 2. Neyman contours in the $\mathcal{B}(B_s^0 \rightarrow \mu^+ \mu^-) - \mathcal{B}(B^0 \rightarrow \mu^+ \mu^-)$ plane for 68.3, 95.5 and 99.7 % coverage. At each coverage value, the inner contours are statistical uncertainty only, while the outer ones include statistical and systematic uncertainties. The construction of these contours makes use of both the dimuon (26.3 fb^{-1}) and the reference channel (15.1 fb^{-1}) datasets [8].

$m_{J/\psi K^\pm}$ while the efficiency relative to $B_{(s)}^0 \rightarrow \mu^+ \mu^-$ is extracted from Monte Carlo (MC) within a fiducial volume defined by $p_T(B) > 8 \text{ GeV}$ and $|\eta_B| < 2.5$. The overall efficiency ratio $R_\varepsilon = \varepsilon_{J/\psi K^\pm} / \varepsilon_{\mu^+ \mu^-}$ is $0.1176 \pm 0.0009 \text{ (stat.)} \pm 0.0047 \text{ (syst.)}$ with the largest contribution to the systematic uncertainties originating from data-MC discrepancies in the BDT input quantities. A correction of 2.7% has been applied to R_ε to account for the effective B_s^0 lifetime.

Due to the limited mass resolution the overlapping B_s^0 and B^0 peaks are statistically separated by an unbinned maximum likelihood fit to the $m_{\mu^+ \mu^-}$ distributions in four BDT bins. The signal and $B \rightarrow hh'$ distributions are modelled by three double-Gaussian PDFs, each with a common mean, while the background is described by a first-order polynomial (combinatorial background) in combination with an exponential distribution ($b \rightarrow \mu^+ \mu^- X$ and semi-leptonic background) whose shape parameters and normalisations are obtained from data (Fig. 1).

For the Run 2 data, yields of $N_s = 80 \pm 22$ $B_s^0 \rightarrow \mu^+ \mu^-$ and $N_d = -12 \pm 20$ $B^0 \rightarrow \mu^+ \mu^-$ events are extracted, consistent with SM expectations of $N_s^{SM} = 91$ and $N_d^{SM} = 10$, respectively. Employing a Neyman construction (Fig. 2) a branching fraction of $\mathcal{B}(B_s^0 \rightarrow \mu^+ \mu^-) = (3.21^{+0.96}_{-0.91} \text{ (stat.)}^{+0.49}_{-0.30} \text{ (syst.)}) \times 10^{-9}$ and an upper limit of $\mathcal{B}(B^0 \rightarrow \mu^+ \mu^-) < 4.3 \times 10^{-10}$ at 95% CL are obtained. A combination of the likelihood contours of the Run 2 (2015 and 2016) and Run 1 results (Fig. 3) is compatible with the SM at 2.4σ level and results in $\mathcal{B}(B_s^0 \rightarrow \mu^+ \mu^-) = (2.8^{+0.8}_{-0.7}) \times 10^{-9}$ and $\mathcal{B}(B^0 \rightarrow \mu^+ \mu^-) < 2.1 \times 10^{-10}$ at 95% CL.

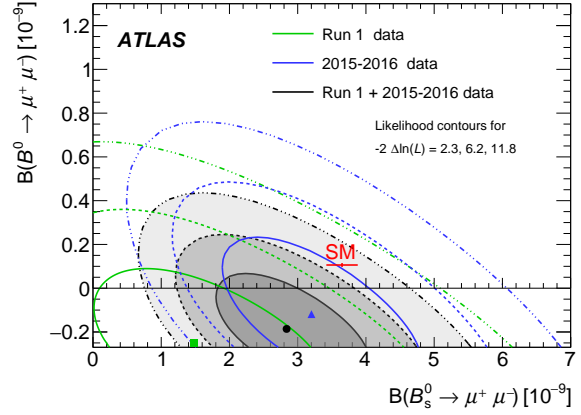


FIG. 3. Likelihood contours for the combination of the Run 1 and 2015-2016 Run 2 results (shaded areas). The contours are obtained with the combination of the two analyses likelihood, for values of $-2 \Delta \ln \mathcal{L}$ equal to 2.3, 6.2 and 11.8. The contours for the individual Run 2 2015-2016 and Run 1 results are overlaid. The SM predictions and their uncertainties are included [8].

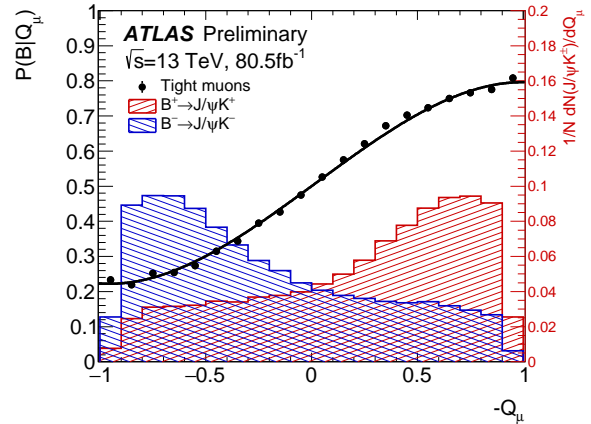


FIG. 4. Cone charge distributions, Q_μ , for tight muons, shown for the continuous distribution. For each plot, in red (blue), the normalised B^+ (B) cone charge distribution is shown (corresponding to the right axis scale). Superimposed is the distribution of the tag-probability, $P(B|Q_\mu)$, as a function of the cone charge, derived from a data sample of $B^\pm \rightarrow J/\psi K^\pm$ and defined as the probability to have a B^+ meson (on the signal-side) given a particular cone charge Q_μ . The fitted parametrization, shown in black, is used as the calibration curve to infer the probability to have a B_s^0 or B^0 meson produced at production in the decays to $B_s^0 \rightarrow J/\psi \phi$ [12].

III. CP-VIOLATION IN $B_s^0 \rightarrow J/\psi \phi$

In the SM, the CP violating phase ϕ_s in the $B_s^0 \rightarrow J/\psi \phi$ decay (with $J/\psi \rightarrow \mu^+ \mu^-$ and $\phi \rightarrow K^+ K^-$) is small and can be predicted to $\phi_s \approx -2\beta_s = -0.0363^{+0.016}_{-0.0015} \text{ rad}$ [9]. The ATLAS Run 1 mea-

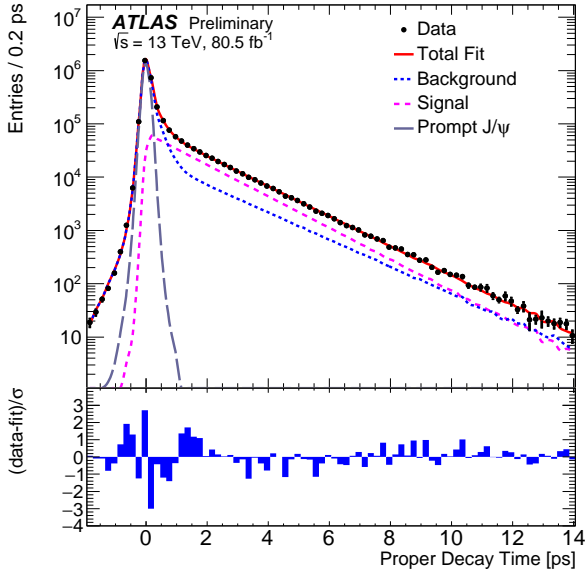


FIG. 5. Proper decay time fit projection for the $B_s^0 \rightarrow J/\psi\phi$ sample. The red line shows the total fit, while the magenta dashed line shows the total signal. The total background is shown as a blue dashed line with a long-dashed grey line showing the prompt J/ψ background. Below the figure is a ratio plot that shows the difference between each data point and the total fit line divided by the statistical and systematic uncertainties summed in quadrature of that point [12].

surement [11] of $\phi_s = -0.090 \pm 0.078$ (stat.) ± 0.041 (syst.) rad and of the decay width difference $\Delta\Gamma_s = 0.085 \pm 0.011$ (stat.) ± 0.007 (syst.) ps $^{-1}$ agrees with SM expectations ($\Delta\Gamma_s = 0.087 \pm 0.021$ ps $^{-1}$ in SM [10]) and is consistent with results from other experiments.

The ATLAS Run-2 $B_s^0 \rightarrow J/\psi\phi$ measurement [12] uses 80.5 fb $^{-1}$ of 13 TeV data taken in 2015-2017 selected by multiple triggers based on $J/\psi \rightarrow \mu^+\mu^-$ decays with muon- p_T thresholds of 4 or 6 GeV. In order to extract the flavour of the decaying B_s^0 (or \bar{B}_s^0) opposite-side taggers which rely on the p_T -weighted charge of tracks Q_x inside a cone around either an electron, a muon or a b -jet are used. The taggers are calibrated on self-tagging $B^\pm \rightarrow J/\psi K^\pm$ events and yield a total tagging power of $1.65 \pm 0.01\%$ with the tight muon tagger contributing $0.86 \pm 0.01\%$, about half of the tagging power (Fig. 4).

An unbinned maximum likelihood fit based on the B_s^0 properties (p_T mass and mass uncertainty, proper decay time (Fig. 5) and uncertainty, the B_s^0 -flavour tagging probability $p(B|Q_x)$ and the transversity angles $\Omega(\theta_T, \phi_T, \psi_T)$, defined in [12], is employed to extract nine signal parameters. For Run 2 data only, values of $\phi_s = -0.068 \pm 0.038$ (stat.) ± 0.018 (syst.) rad and $\Delta\Gamma_s = -0.067 \pm 0.005$ (stat.) ± 0.002 (syst.) ps $^{-1}$

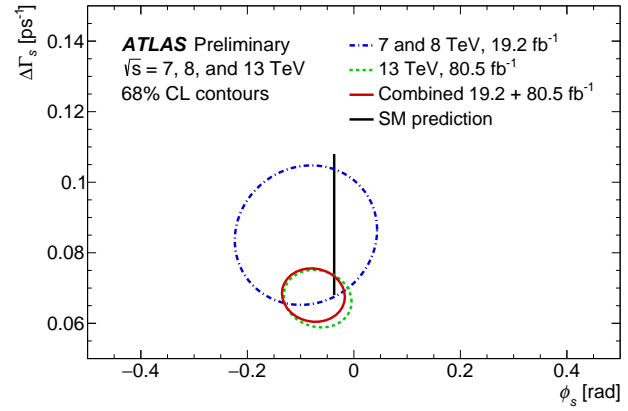


FIG. 6. Likelihood 68% confidence level contours in the $\phi_s - \Delta\Gamma_s$ plane, showing ATLAS results for 7 TeV and 8 TeV data (blue dashed-dotted curve), for 13 TeV data (green dashed curve) and for 13 TeV data combined with 7 TeV and 8 TeV (red solid curve) data. In all contours the statistical and systematic uncertainties are combined in quadrature and correlations are taken into account [12].

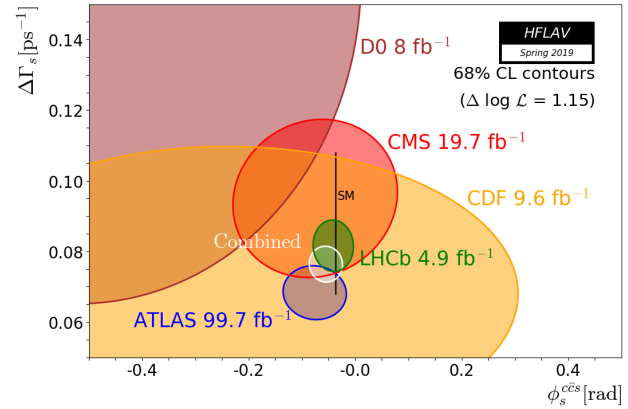


FIG. 7. Likelihood 68% confidence level contours in the $\phi_s - \Delta\Gamma_s$ plane, including results from D0 (brown), CDF (yellow), LHCb (green) and CMS (red). The brown contour with blue edge shows the ATLAS result for 13 TeV combined with 7 TeV and 8 TeV. The statistical and systematic uncertainties are combined in quadrature. A preliminary HFLAV combination is shown by the white contour [13].

(Fig. 6) are obtained.

The combined ATLAS Run 1 and Run 2 result yields $\phi_s = -0.076 \pm 0.034$ (stat.) ± 0.019 (syst.) rad and $\Delta\Gamma_s = -0.068 \pm 0.004$ (stat.) ± 0.003 (syst.) ps $^{-1}$ which are consistent with the SM expectations as well as results from other experiments (Fig. 7). A preliminary HFLAV average [13] results in $\phi_s = -0.055 \pm 0.021$ rad and $\Delta\Gamma_s = -0.0764_{-0.0033}^{+0.0034}$ ps $^{-1}$.

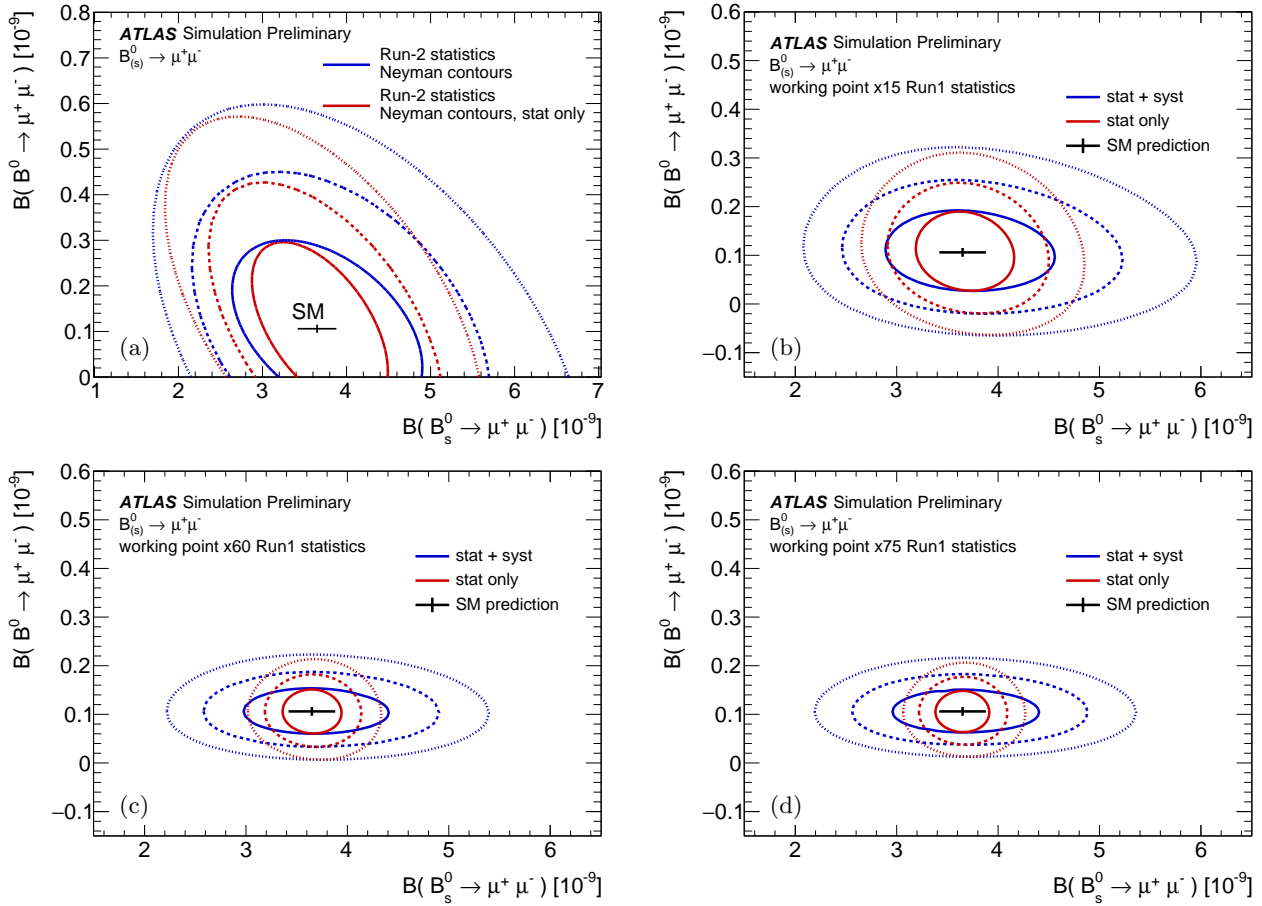


FIG. 8. (a): Comparison of 68.3% (solid), 95.5% (dashed) and 99.7% (dotted) confidence level contours obtained exploiting the 2D Neyman belt construction for the full LHC Run 2 case [15]. Red contours are statistical only; blue contours include systematics uncertainties from the ATLAS Run 1 analysis [5] extrapolated to Run 2 statistics. The black points show the SM theoretical prediction and its uncertainty [4].

(b) - (d): Comparison of confidence level profiled likelihood ratio contours for (b) the “conservative”, (c) the “intermediate” and (d) the “high-yield” HL-LHC extrapolation with $\times 15$, $\times 60$ and $\times 75$ the Run 1 statistics for the (10 GeV, 10 GeV), the (6 GeV, 10 GeV) and the (6 GeV, 6 GeV) dimuon trigger scenarios, respectively [15].

IV. HIGH-LUMINOSITY LHC PROSPECTS

The branching fraction measurement of the very rare decays $B_s^0 \rightarrow \mu^+ \mu^-$ and $B^0 \rightarrow \mu^+ \mu^-$ will benefit from the increased statistics and the improved invariant mass resolution at the HL-LHC. The separation of the B_s^0 and B^0 mass peaks increases by a factor of 1.65 (1.5) to 2.3σ (1.3σ) in the barrel (end-cap) region compared to Run 1 [14].

The projection of the ATLAS detector performance for measuring $\mathcal{B}(B_{(s)}^0 \rightarrow \mu^+ \mu^-)$ with the expected datasets during the full LHC Run 2 (130 fb^{-1}) and at the HL-LHC (3000 fb^{-1}) [15] using pseudo-MC experiments is based on the likelihood of the Run 1 analysis. The signal statistics estimate for the Run 2 scenario applies scaling factors for the integrated luminosity, the cross-section increase due to the higher center-of-

mass energy of 13 TeV and the muon pair selection with topological triggers with $(p_T(\mu_{1,2}) > 6 \text{ GeV})$ or $(p_T(\mu_1) > 6 \text{ GeV}, p_T(\mu_2) > 4 \text{ GeV})$ thresholds resulting in 7 times the number of signal events in Run 1. The contours of the 2-dimensional Neyman construction (Fig. 8 (a)) include the external systematic uncertainties on the b -quark fragmentation fractions f_s/f_d and $\mathcal{B}(B^\pm \rightarrow J/\psi K^\pm)$ which were kept the same as in the Run 1 analysis as well as internal ones like the fit shapes and efficiencies which were scaled according to the increase in statistics. For the HL-LHC case three potential trigger scenarios are considered: two muons with $p_T > 10 \text{ GeV}$ (“conservative”), one muon with $p_T > 10 \text{ GeV}$ and another with $p_T > 6 \text{ GeV}$ (“intermediate”) as well as two muons with $p_T > 6 \text{ GeV}$ (“high yield”) providing 15, 60 and 75 times the Run 1 statistics, respectively. The profile likelihood contours of pseudo-experiments based again

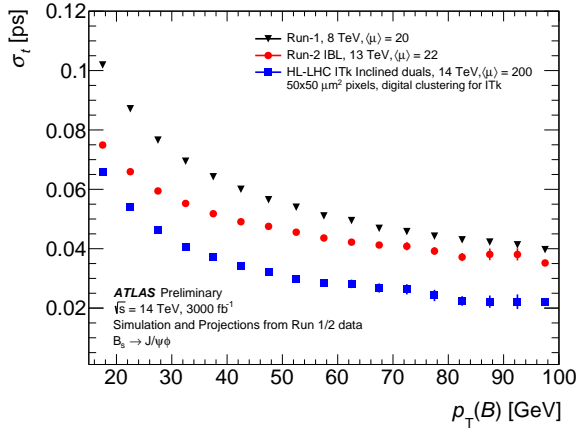


FIG. 9. Dependence of the proper decay time resolution of the B_s^0 meson of the signal $B_s^0 \rightarrow J/\psi\phi$ decay on B_s^0 p_T . Per-candidate resolutions corrected for scale-factors are shown, comparing the performance in Run 1 (ID), Run 2 (IBL) and upgrade HL-LHC (ITk) MC simulations. All samples use 6 GeV muon p_T cuts [17].

on the likelihood of the Run 1 analysis demonstrate the increased sensitivity of the ATLAS detector for $\mathcal{B}(B_s^0 \rightarrow \mu^+\mu^-)$ and $\mathcal{B}(B^0 \rightarrow \mu^+\mu^-)$ at the HL-LHC (Fig. 8 (b)-(d)). The uncertainty on the f_s/f_d value, conservatively taken as 8.3% from the ATLAS measurement [16], dominates the systematic uncertainty contributions on $\mathcal{B}(B_s^0 \rightarrow \mu^+\mu^-)$.

The prospects of measuring the CP-violating phase ϕ_s and the B_s^0 decay width difference $\Delta\Gamma_s$ using $B_s^0 \rightarrow J/\psi\phi$ decays at the HL-LHC (3000 fb^{-1}) [17] have been explored by pseudo-MC experiments based on the Run 1 $B_s^0 \rightarrow J/\psi\phi$ analysis using similar trigger scenarios as in the $B_{(s)}^0 \rightarrow \mu^+\mu^-$ HL-LHC study, yielding a B_s^0 signal statistics increase of $\times 18$, $\times 60$ and $\times 100$ w.r.t. the yield obtained in 2012 data for the “conservative”, “intermediate” and “high-yield” scenarios, respectively. The sensitivity to ϕ_s as well as to $\Delta\Gamma_s$ is improved considerably by the detector upgrades, especially the proper time resolution σ_t (Fig. 9). In the calculation of the expected uncertainties on ϕ_s and $\Delta\Gamma_s$ the number of B_s^0 signal events and the proper time resolution σ_t are assumed to scale with the integrated luminosity while the B_s^0 flavour tagging power – conservatively – is not scaled. The systematic uncertainties (likelihood fit model description, B_s^0 flavor tagging calibration, detector acceptance description, detector alignment, peaking background contributions) are expected to improve with increased statistics as well, providing estimates of $\delta_{\phi_s}^{syst} \approx 0.003$ rad and $\delta_{\Delta\Gamma_s}^{syst} \approx 0.0005$ ps^{-1} for an integrated luminosity of 3000 fb^{-1} . The improvement in the statistical uncertainties obtained w.r.t. the Run 1 result are factors 9 to 20 for ϕ_s , up to 7 times smaller than the SM prediction for ϕ_s , and factors 4 to 10 for

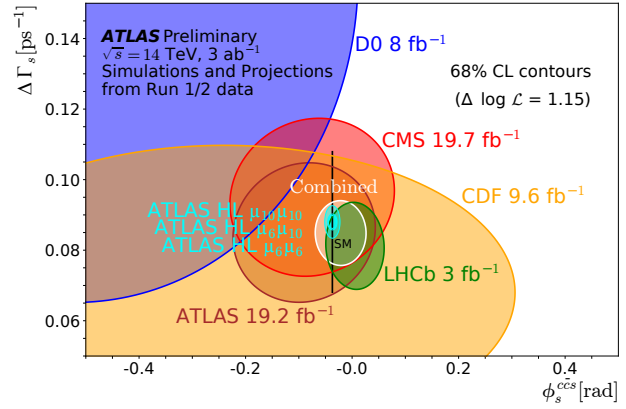


FIG. 10. Experimental summary of the $\phi_s - \Delta\Gamma_s$ measurements with superimposed ATLAS HL-LHC extrapolations, including both the projected statistical and systematic uncertainties [17].

$\Delta\Gamma_s$. The 68% CL contours for the three scenarios (Fig. 10) include the combination of statistical and systematic uncertainties.

V. SUMMARY

Measurements of rare decays and CP-violation by the ATLAS collaboration have been presented. The results for $\mathcal{B}(B_s^0 \rightarrow \mu^+\mu^-)$ and the search for the decay $\mathcal{B}(B^0 \rightarrow \mu^+\mu^-)$ with 36.2 fb^{-1} of Run-2 data agree with the Standard Model and other measurements. There is no sign for the decay $B^0 \rightarrow \mu^+\mu^-$ in ATLAS data, but ATLAS will add approximately data taken in 2017 and 2018 to the analysis (≈ 107 fb^{-1}).

The ATLAS measurement of the CP-violating phase ϕ_s and the B_s^0 decay width difference $\Delta\Gamma_s$ provides a single measurement precision comparable to that of the LHCb experiment and reaches the sensitivity to test the Standard Model prediction. About 60 fb^{-1} of data taken in 2018 will be added to the analysis in the future.

Both analyses will profit considerably from the increased statistics expected from the 3000 fb^{-1} of HL-LHC data as well as detector improvements providing better mass and proper decay time resolutions. This will allow more stringent tests of the Standard Model.

ACKNOWLEDGMENTS

This work was partially supported by grants of the German Federal Ministry of Education and Research (BMBF) and the German Helmholtz Alliance “Physics at the Terascale”.

-
- [1] ATLAS Collaboration, *The ATLAS Experiment at the CERN Large Hadron Collider*, 2008 JINST 3 S08003
- [2] L. Evans and P. Bryant (editors), *LHC Machine*, 2008 JINST 3 S08001
- [3] G. Apollinari, I. Béjar Alonso, O. Brüning, P. Fes-
sia, M. Lamont, L. Rossi, L. Tavian (editors), *High-
Luminosity Large Hadron Collider (HL-LHC)*, *Techni-
cal Design Report V. 0.1*, CERN Yellow Reports
Vol. 4/2017, CERN-2017-007-M (CERN, Geneva,
2017) [<https://cds.cern.ch/record/2284929>]
- [4] C. Bobeth et al., $B_{s,d}^0 \rightarrow \ell^+ \ell^-$ in the Standard
Model with Reduced Theoretical Uncertainty, *Phys.*
Rev. Lett. 112 (2014) 101801
- [5] ATLAS Collaboration, *Study of the rare decays of B_s^0
and B^0 into muon pairs from data collected during the
LHC Run 1 with the ATLAS detector*, *Eur. Phys. J. C*
(2016) 76:513
- [6] CMS and LHCb Collaborations, *Observation of the
rare $B_s^0 \rightarrow \mu^+ \mu^-$ decay from the combined analysis of
CMS and LHCb data*, *Nature*, **522**, 2015
- [7] LHCb Collaboration, *Measurement of the $B_s^0 \rightarrow$
 $\mu^+ \mu^-$ Branching Fraction and Effective Lifetime and
Search for $B^0 \rightarrow \mu^+ \mu^-$ Decays*, *Phys. Rev. Lett.* 118
(2017) 191801
- [8] ATLAS Collaboration, *Study of the rare decays of
 B_s^0 and B^0 mesons into muon pairs using data col-
lected during 2015 and 2016 with the ATLAS detector*,
JHEP04 (2019) 098
- [9] J. Charles et al., *Predictions of selected flavour ob-
servables within the standard model*, *Phys. Rev. D* **84**
(2011) 033005
- [10] A. Lenz and U. Nierste, *Numerical updates of life-
times and mixing parameters of B mesons*, (2011),
[arXiv:1102.4274](https://arxiv.org/abs/1102.4274)
- [11] ATLAS Collaboration, *Measurement of the CP-
violating phase ϕ_s and the B_s^0 meson decay width
difference with $B_s^0 \rightarrow J/\psi \phi$ decays in ATLAS*,
JHEP 08 (2016) 147
- [12] ATLAS Collaboration, *Measurement of the CP
violation phase ϕ_s in $B_s^0 \rightarrow J/\psi \phi$ decays
in ATLAS at 13 TeV*, ATLAS-CONF-2019-009,
[<https://cds.cern.ch/record/2668482>]
- [13] Heavy Flavor Averaging Group, Preliminary combi-
nation of ϕ_s vs. $\Delta\Gamma_s$ results, spring 2019, CERN
seminar presentation by F. Dordei, 2019-05-07,
[<https://hflav.web.cern.ch/>]
- [14] ATLAS Collaboration, *Expected performance
for an upgraded ATLAS detector at High-
Luminosity LHC*, ATL-PHYS-PUB-2016-026
[<https://cds.cern.ch/record/2223839>]
- [15] ATLAS Collaboration, *Prospects for the
 $\mathcal{B}(B_{(s)}^0 \rightarrow \mu^+ \mu^-)$ measurements with the AT-
LAS detector in Run 2 LHC and HL-LHC
data campaigns*, ATL-PHYS-PUB-2018-005,
[<https://cds.cern.ch/record/2317211>]
- [16] ATLAS Collaboration, *Determination of the ratio of
b-quark fragmentation fractions f_s/f_d in pp collisions
at $\sqrt{s} = 7$ TeV with the ATLAS detector*, *Phys. Rev.*
Lett. 115, 262001 (2015)
- [17] ATLAS Collaboration, *CP-violation measure-
ment prospects in the $B_s^0 \rightarrow J/\psi \phi$ chan-
nel with the upgraded ATLAS detector at
the HL-LHC*, ATLAS-PHYS-PUB-2018-041,
[<https://cds.cern.ch/record/2649881>]